SCIENCE CHINA
Technological Sciences

• Article •

March 2017 Vol.60 No.3: 345–354
doi: 10.1007/s11431-016-0604-3

Multi-objective optimization of cooling air distribution of grate cooler with different inlet temperatures by using genetic algorithm

SHAO Wei, CUI Zheng & CHENG Lin*

Institute of Thermal Science and Technology, Shandong University, Jinan 250061, China

Received August 12, 2016; accepted November 28, 2016; published online January 23, 2017

The paper discussed a multi-objective optimization model of the cooling air distribution of a grate cooler according to the analogy of a cross-flow heat exchanger and entropy-generation minimization analysis. The modified entropy generation numbers caused by heat transfer and flowing resistance are regarded as objective functions, and are simultaneously optimized by a genetic algorithm. A test is conducted to validate the model. The final optimal cooling air distribution is decided by energy consumed through cooling fans minimization. Next, two schemes are investigated for inducing exhaust air of 70°C–100°C in a chimney to cool the middle and front parts of the grate cooler. Based on each scheme, sensitive analyses of cooling air inlet temperatures are conducted. The results show that the minimum energy consumption of cooling fans increases by 121.04%, and the thermal efficiencies of the grate cooler vary no more than 1.66% when inducing the exhaust air into the middle part of the grate cooler. The minimum energy consumption of cooling fans slightly varies and thermal efficiencies of grate coolers vary no more than 0.51% when inducing exhaust air to the front part of the grate cooler. It is more effective and economical to induce exhaust air at any temperature to the front part of the grate cooler.

cooling air distribution, grate cooler, multi-objective genetic algorithm, entropy generation

Citation: Shao W, Cui Z, Cheng L. Multi-objective optimization of cooling air distribution of grate cooler with different inlet temperatures by using genetic algorithm. Sci China Tech Sci, 2017, 60: 345–354, doi: 10.1007/s11431-016-0604-3

1 Introduction

The cement production industry is one of the most energy intensive industries. In most regions, energy expenditure accounts for 50%–60% of the direct production cost of cement [1]. In China, the energy consumption of cement industry accounts for over 10% of the country's industrial final energy consumption [2]. The cement production technique includes preheating-decomposing system, calcination system and cooling system. A grate cooler is the key equipment contributing to the rapid cooling of clinker and in recovering of heat in cement production. Moving packed bed is usually used which includes fixed grate plates and moving grate plates. High-temperature clinker (1400°C) falls onto the grate plates from a rotary kiln and forms a layer with a certain thickness. From beneath the grate plates, cooling air flows vertically through the horizontally moving clinker layer to cool it, as shown in Figure 1. Despite several efforts being made in the past two decades, relevant studies indicate that there is still large potential for improving energy efficiency of cement production [3].

Many investigators have focused on increasing the performance of grate coolers. Caputo et al. [4] proposed a dynamic clinker cooling simulation method, which applies the convective heat transfer principle in the grate cooler. Touil et al. [5] proposed a clinker cooling model based on mass and energy balance, analyzed the exergy balance and entropy generation of the cooling process, and discussed the effects of

* Corresponding author (email: cheng@sdu.edu.cn)

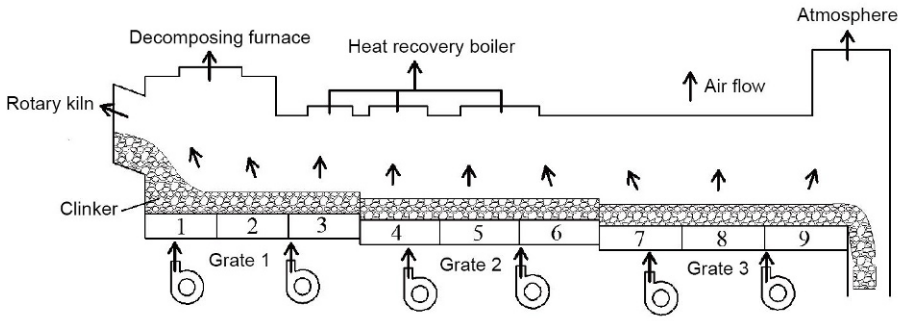

Figure 1 Structure of grate cooler and clinker cooling principle.

cooling air temperature and the number of chambers in entropy generation. Madlool et al. [6] reviewed the analyses of exergy balance and efficiency in cement production, and indicated that exergy analysis is crucial for increasing system efficiency. Liu et al. [7] analyzed the energy flow model of cement production and concluded that the cooling of the clinker is the second factor affecting heat efficiency. However, most studies on grate coolers focus on increasing the heat efficiency by exergy or energy analyses. To our knowledge, there are few study that focuses on the cooling air distribution in grate coolers.

The main factors for evaluating the performance of cooling air system are cooling efficiency and flowing resistance. Furthermore, both are closely related to the energy consumption of cooling fans. Nevertheless, cooling efficiency and flowing resistance are contradictory to each other, considering the velocities of the cooling air, which cause a multi-objective optimization problem. Pareto optimality is an efficient method to handle multi-objective optimization. An efficient approach to manage optimization of multi-objective design problems is to employ a genetic algorithm. Multi-objective optimization involves determining a trade-off among the multiple conflicting objectives. It is widely used in analyzing energy systems and aims to improve exergy efficiency [8–12]. Seijo et al. [13] proposed a multi-objective theory of optimizing plant performance with three goals: to maximize electrical production, minimize fuel consumption, and maximize the amount of heat used in the slurry process. Usually, a specific heating load, coefficient of performance, and thermo-economic criterion are simultaneously considered as objective functions to be maximized in heat pump cycle optimization [14–16]. In the study of grate cooler, Caputo et al. [17] proposed a clinker cooling model by formulating a cross-flow heat exchanger theory and optimized the structure of a heat recovery system and its operating parameters. Caputo et al. [18] optimized the structure and configuration of a grate cooler according to total investment minimization, and the annual cost decreased by 10%–25%. However, few studies have focused on the optimization of cooling air distribution of a grate cooler, which directly affects energy consumption of cooling fans.

In this study, a multi-objective optimization model of cooling air distribution of a grate cooler is proposed to obtain optimal cooling air distribution based on simultaneous entropy generations through heat transfer and flowing resistance minimization. The Pareto front of these two objectives is obtained by solving the proposed model, and each point on the curve corresponds to an optimum location and a set of operation parameters. The final optimal cooling air distribution is obtained according to energy consumed through cooling fans minimization. Exhaust air of 70°C–100°C is usually induced in a chimney to cool the clinker again (cycle air technique), which is expected to recover the low-temperature heat sources in cement production. Therefore, two schemes of inducing exhaust air in a chimney are conducted. Based on each scheme, sensitive analyses of the inlet temperature of cooling air, varying from 30°C to 100°C with 10°C interval, are conducted and discussed (Figure 2).

2 Model framework

2.1 Overview

The second law of thermodynamics indicates that all natural processes are irreversible. Entropy generation analysis is the most common and fundamental for thermodynamic optimization. Heat is transferred between vertically flowing cooling air and horizontally moving clinker layers in a grate cooler, which can approximate to cross-flow heat exchanger. Therefore, the irreversible loss in grate cooler includes entropy generation through heat transfer and flowing resistance. The description of entropy generation rate for two fluids (fluids 1 and 2) is given by [19]

$$\dot{S}_{\text{gen}} = \left(mC_p\right)_1 \ln\left(\frac{t_{1,\text{out}}}{t_{1,\text{in}}}\right) + \left(mC_p\right)_2 \ln\left(\frac{t_{2,\text{out}}}{t_{2,\text{in}}}\right) - \left(mR_g\right)_1 \ln\left(\frac{P_{1,\text{out}}}{P_{1,\text{in}}}\right) - \left(mR_g\right)_2 \ln\left(\frac{P_{2,\text{out}}}{P_{2,\text{in}}}\right), \quad (1)$$

where m is the mass flow rate, kg/s; C_p is the heat capacity, J/(kg K); t is the temperature, °C; P is the pressure, Pa; R_g is the air gas constant, 287 J/(kg K); Owing to the existence of

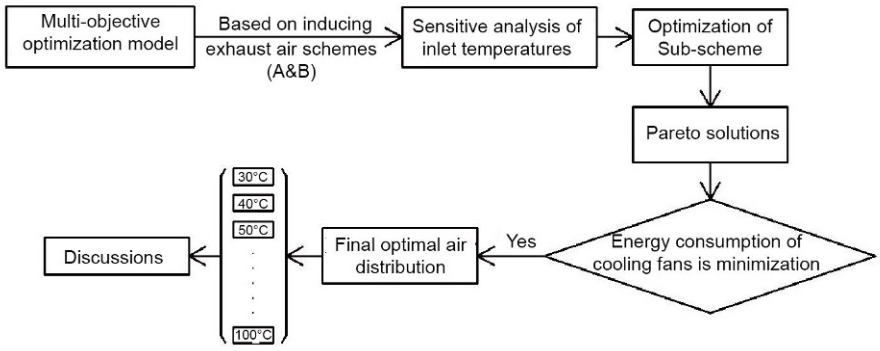

Figure 2 Flow chart of the study.

"entropy generation paradox" [20], to nondimensionalize, the entropy generation rate will divide Q/t_0, which is called the modified entropy generation number [21–23].

The research is based on a grate cooler in a 5000 t/d cement plant that includes nine air chambers. The clinker cooling process is modeled through a series of stages, as shown in Figure 3.

2.2 Analysis of entropy generation caused by heat transfer

If the internal thermal conductivity resistance cannot be ignored, the integrated heat transfer coefficient between clinker particles and cooling air in stage i is given by [24]

$$k_i = \frac{1}{\frac{1}{h_i} + \frac{\varphi r}{\lambda_s}}, \tag{2}$$

where k is integrated heat transfer coefficient, W/(m^2 K); h is the convective heat transfer coefficient, W/(m^2 K); φ is the paricle shape correction factor; r is the particle heating depth, m; λ is the thermal conductivity, W/(m K). The convective heat transfer coefficient between the clinker particles and cooling air is given by [24]

$$\mathrm{Nu}_i = 2 + 1.8\mathrm{Pr}_i^{\frac{1}{3}}\mathrm{Re}_i^{\frac{1}{2}}, \tag{3}$$

$$\mathrm{Nu}_i = h_i D_p / \lambda_s, \tag{4}$$

$$\mathrm{Re}_i = V_i D_p / v_{gi}, \tag{5}$$

where D_p is the average diameter of clinker particle, m; V is the superficial velocity of cooling air, m/s; v_g is the dynamic viscosity of air, kg/(m s); The effective heat transfer area between the clinker particles and cooling air is calculated as [24]

$$A_i = \frac{6U_i(1-\varepsilon)}{D_p}, \tag{6}$$

where U_i=$L_i YH_j$, U is the volume of clinker, m^3; ε is the porosity of clinker; L is the length of chamber, m; Y is the width of the grate cooler, m; H is the thickness of clinker, m. By applying the analogy of cross-flow heat exchanger, the heat transfer rate between the clinker and cooling air is obtained as [17]

$$Q_i = \left(t_{2(i-1)} - t_{a0}\right)\frac{1-q_i}{\frac{1}{C_{a,i}} - \frac{q_i}{C_s}}, \tag{7}$$

where

$$q_i = \exp\left(k_i A_i \left(C_{a,i} - C_s\right) / C_{a,i} C_s\right), \tag{8}$$

$$C_s = m_s C_{ps}, \tag{9}$$

$$C_{a,i} = \rho V_i L_i W C_{pa,i}, \tag{10}$$

where Q is the heat transfer rate, W; C is the heat capacity rate, W/K; The subscripts s and a stand for clinker and cooling air; ρ is the density, kg/m^3. According to the energy balance principle, the outlet temperature of cooling air is given by [17]

$$t_{2i-1} = t_{a0} + \frac{Q_i}{C_{a,i}}. \tag{11}$$

Further, the clinker outlet temperature is given by [17]

$$t_{2i} = t_{2(i-1)} - \frac{Q_i}{C_s}. \tag{12}$$

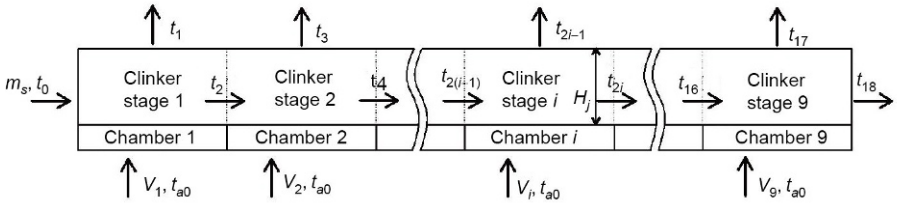

Figure 3 Clinker cooling in multiple crosscurrent contacting beds.

The entropy generation rate caused by heat transfer is given by

$$S_{\mathrm{gen},\Delta T} = C_s \ln\left(\frac{t_{18}}{t_{s,\mathrm{in}}}\right) + \sum_{i=1}^{9} C_{a,i} \ln\left(\frac{t_{2i-1}}{t_{a0}}\right). \tag{13}$$

Moreover, the modified entropy generation number is given by

$$N_{s,\Delta T} = \frac{S_{\mathrm{gen},\Delta T} \cdot t_{a0}}{\sum_{i=1}^{9} Q_i}. \tag{14}$$

2.3 Analysis of entropy generation caused by flowing resistance

The pressure drop in packed bed such as clinker is given by the following Ergun equation [24]:

$$\frac{\Delta P_i}{H_j} = \frac{150\mu_i}{D_p^2} \cdot \frac{(1-\varepsilon)^2}{\varepsilon^3} \cdot V_i + \frac{1.75\rho_i}{D_p} \cdot \frac{1-\varepsilon}{\varepsilon^3} \cdot V_i^2, \tag{15}$$

where μ is the kinematic viscosity of air, kg/(m s). In addition, the entropy generation rate caused by pressure drop is obtained by

$$S_{\mathrm{gen},\Delta P} = m_i R_g \sum_{i=1}^{9} \ln\left(1 + \frac{\Delta P_i}{P_{\mathrm{out}}}\right), \tag{16}$$

where $m_i = \rho V_i L_i W$.

The modified entropy generation number is defined as

$$N_{s,\Delta P} = \frac{S_{\mathrm{gen},\Delta P} \cdot t_{a0}}{\sum_{i=1}^{9} Q_i}. \tag{17}$$

3 Description of the test case

3.1 Boundary conditions and assumptions

The width of the grate cooler is 4 m. The length of the chambers and other related boundary conditions are listed in Table 1.

To simplify the problem, some assumptions are made: the operating conditions of the grate cooler and kiln system are steady; the clinker is distributed uniformly on grates and transverse temperature difference is ignored; clinker particles approximate to spheres and isotropic materials; the clinker moves horizontally, cooling air flows vertically, and there is no sedimentation. Radiative heat transfer in the system is ignored; pressure reference of the system is standard atmospheric pressure.

3.2 Design variables, constraints and objectives

The design variables and their ranges are as follows:

(1) Superficial velocities of cooling air of chambers 1 to 9, ranging from 0.5 to 2.5 m/s;

(2) Thicknesses of clinker layers on grate plates 1 to 3, ranging from 0.5 to 0.9 m.

The objectives and constraints conditions based on the production requirements are described as follows:

Table 1 Other related boundary conditions

Parameters	Values
Length of chamber 1	3.26
Length of chamber 2	3.26
Length of chamber 3	4.48
Length of chamber 4	3.54
Length of chamber 5	4.72
Length of chamber 6	3.93
Length of chamber 7	3.85
Length of chamber 8	4.62
Length of chamber 9	4.23
Mass flow rate of clinker (kg/s)	72.22
Clinker inlet temperature (°C)	1400
Specific heat capacity of clinker (J/(kg K))	920 [18]
Pressure of cooling air outlet (Pa)	–50
Porosity of clinker	0.4 [24]
Average diameter of clinker particles (m)	0.02

$$\begin{cases} MinF\left(V_i, H_j\right) = \left[N_{s,\Delta T}, N_{s,\Delta P}\right], \\ \text{s.t.} \quad t_1 > 1200, \\ \qquad t_6 < 600, \\ \qquad t_{12} < 135, \\ \qquad t_{18} < 95. \end{cases}$$

3.3 Multi-objective genetic algorithm and optimization process

An approach of multi-objective optimization is to determine a Pareto optimal solution set in which the solutions do not dominate each other. It is often considered that Pareto optimal solutions are preferred to single solutions because there are several objectives that are often conflicting in real life [25]. A genetic algorithm is applied to optimize this problem. Figure 4 presents the flow chart of the optimization process.

4 Optimization results of test case

The modified entropy generation numbers caused by heat transfer and pressure drop are minimized simultaneously through multi-objective optimization, and the Pareto front is shown in Figure 5. When the modified entropy generation number caused by heat transfer is maximal, that caused by pressure drop is minimized. Contrastively, when the modified entropy generation number caused by heat transfer is minimal, that caused by pressure drop is maximized. Figure 6(a)–(d) demonstrate the scattered distribution of four design variables in grate plate 1 with population in Pareto front: the superficial velocities in three air chambers and the thickness of clinker layer. Lower and upper bounds of the

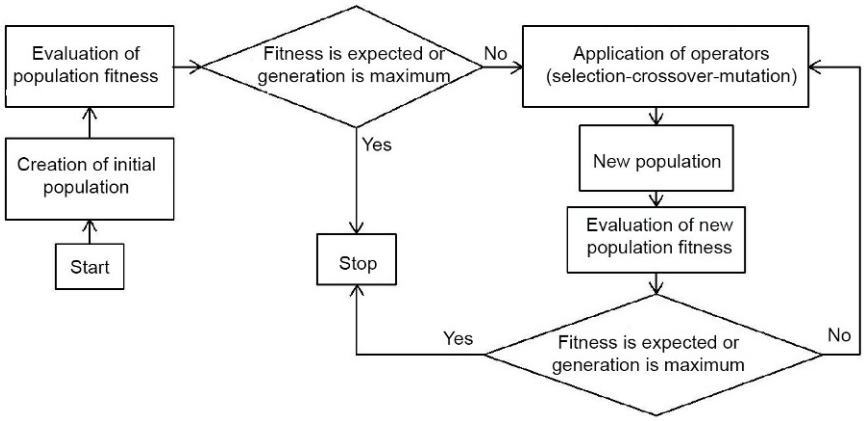

Figure 4 Flow chart of optimization process.

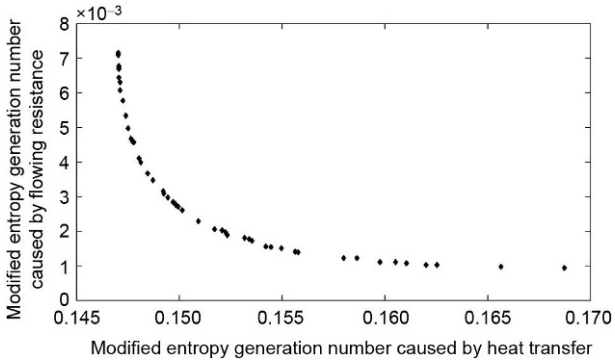

Figure 5 Pareto front for the test case by using genetic algorithm.

variables are represented by the dotted lines. The design variables are observed to have scattered distribution. Therefore, it can be predicted that variations in these variables result in conflict between the two objectives. Variations in other design variables in the left two grate plates have a similar distribution as these four variables. Interestingly, both manufacturers and users, according to their engineering background, could select reasonable cooling air distribution parameters for obtaining optimal Pareto front. In cement production, lower-energy consumption of cooling fans is expected to ensure efficient heat transfer.

5 Sensitive analysis

5.1 Overview

For better usability, the exhaust air is usually induced to cool the clinker again as presented in Section 1. Furthermore, the technique does not require additional fans because the exhaust air can be induced by the existing cooling fans. Figure 7 shows the two schemes of heat recovery. Scheme A involves inducing the exhaust air into the middle part of the grate cooler (chambers 3–6) from which the heat-recovery boiler mainly obtains the heat. Scheme B involves inducing the exhaust air into the front part of the grate cooler (chamber 1) where the temperature difference is quite considerable. Note that both the schemes increase the inlet temperature of cooling air in specific air chambers. Sensitive analyses of inlet temperatures are based on the two inducing schemes. The energy consumption of cooling fans is defined as follows:

$$W = \frac{1}{\eta}\frac{m_a}{\rho_a}\Delta P. \tag{18}$$

The effects of increasing the inlet temperatures of cooling air for minimum energy consumption of cooling fans is discussed in the following sections.

5.2 Optimization of scheme A

The exhaust air is induced to the middle part of the grate cooler so the temperature of the cooling air is a mix of the temperatures of exhaust air (70°C–100°C) and original air (30°C). Different volume distributions will affect the inlet cooling air temperature, and eight subschemes are optimized in scheme A. The sub-schemes are based on the cooling air inlet temperatures in chambers 3–6, and vary from 30°C to 100°C with 10°C intervals. The final optimal cooling air distribution of each subscheme is decided according to energy consumption of cooling fans minimization, as presented in Table 2. Figure 8(a) presents the variation in minimum energy consumed by the cooling fans with the inlet temperatures of cooling air. The minimum energy consumption of cooling fans increases by 121.04%, whereas the inlet temperature of cooling air increases from 30°C to 100°C. The thermal efficiency of the grate cooler is defined as the ratio of heat recovered (including secondary air, tertiary air and air flowing to the heat recovery boiler, see Figure 7) and the total heat into the system as shown below:

$$\eta_g = \frac{\text{Heat recovered}}{\text{Total heat into the system}} \times 100\%. \tag{19}$$

The variation in the thermal efficiency of the grate cooler with the cooling air inlet temperatures is shown in Figure 8(b). There are slight differences among the thermal

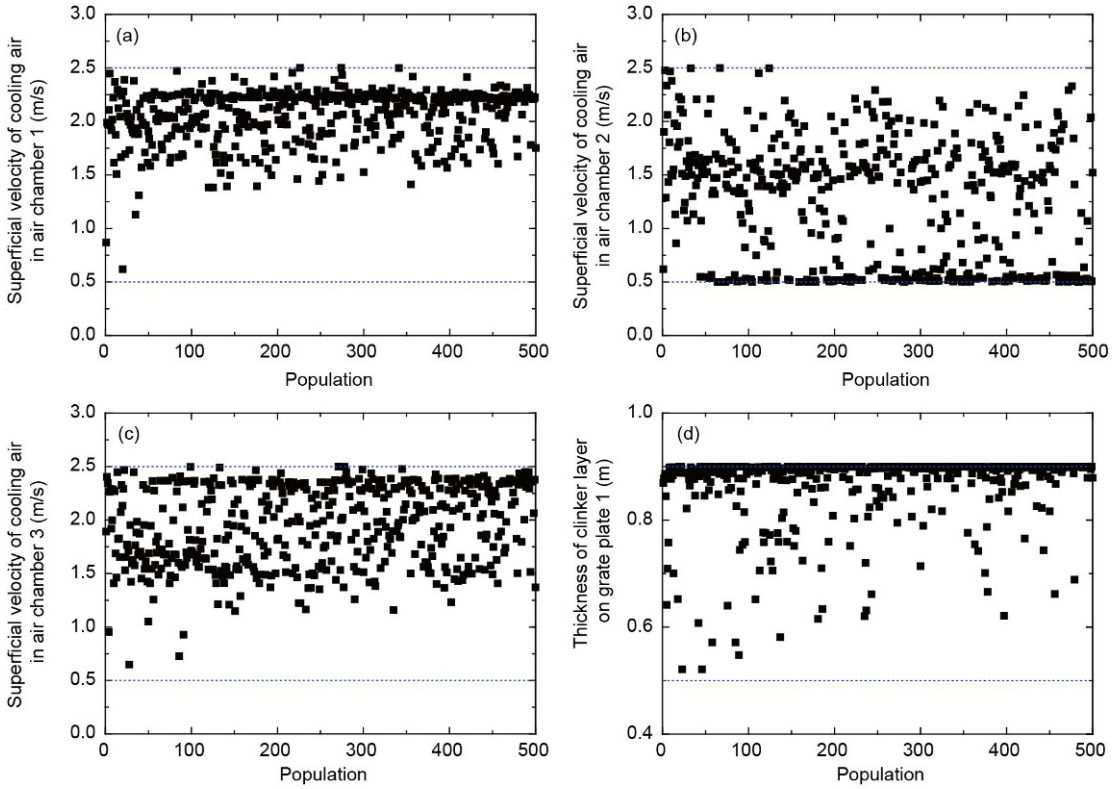

Figure 6 (Color online) Scatter distribution of superficial velocities in chamber 1 (a), chamber 2 (b), chamber 3 (c) and thickness of clinker layer on grate plate 1 (d) with population in Pareto front.

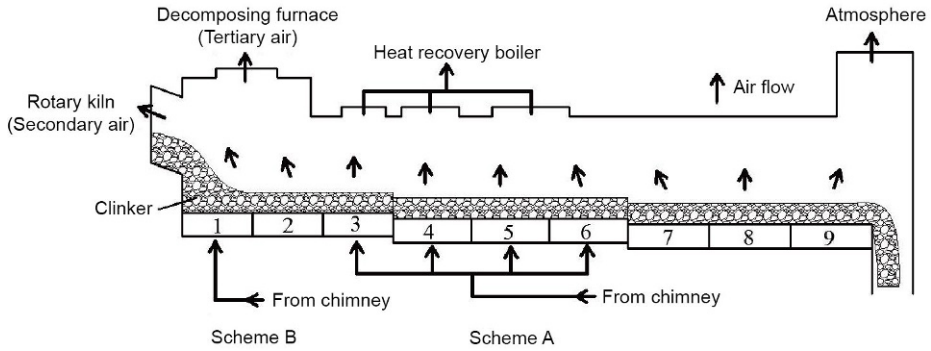

Figure 7 Two schemes of inducing exhaust air in a chimney to cool clinker again.

Table 2 Optimal air distribution of subschemes in scheme A

Cooling air temperature (°C)	Mass flow rate of chamber 1 (kg/s)	Mass flow rate of chamber 2 (kg/s)	Mass flow rate of chamber 3 (kg/s)	Mass flow rate of chamber 4 (kg/s)	Mass flow rate of chamber 5 (kg/s)	Mass flow rate of chamber 6 (kg/s)	Mass flow rate of chamber 7 (kg/s)	Mass flow rate of chamber 8 (kg/s)	Mass flow rate of chamber 9 (kg/s)
30	25.05	22.02	30.93	18.45	23.45	18.90	12.86	12.33	12.89
40	26.00	23.32	28.77	19.31	28.94	19.59	13.92	12.53	15.29
50	25.24	23.59	34.61	19.02	28.79	21.93	10.58	13.70	13.66
60	24.76	22.03	33.41	20.76	28.61	22.89	13.32	14.08	14.93
70	27.37	21.46	33.60	22.42	29.38	23.09	12.38	14.87	13.52
80	28.05	24.75	33.74	25.17	30.26	22.58	11.15	14.89	13.34
90	27.35	27.28	39.53	24.91	33.53	25.07	10.96	15.36	14.92
100	32.26	26.57	39.96	24.95	33.26	24.15	15.39	15.21	15.71

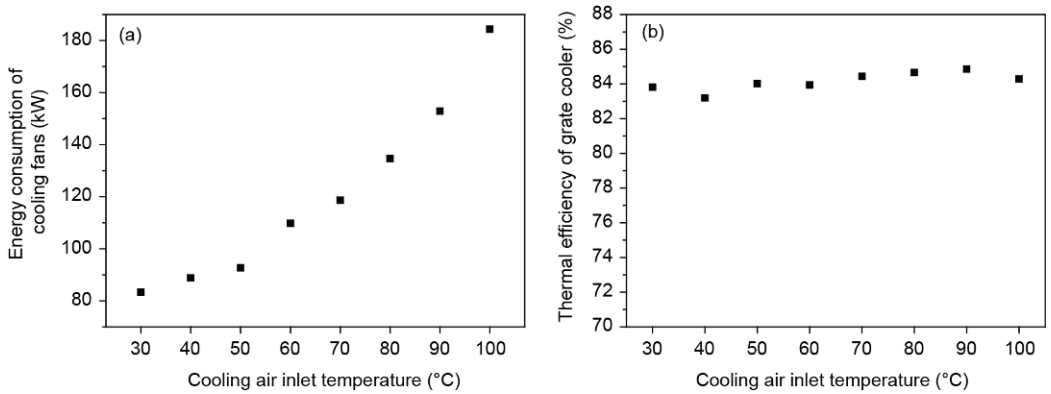

Figure 8 The variation of two key parameters. (a) Minimum energy consumption of cooling fans; (b) thermal efficiency of grate cooler with cooling air inlet temperature in scheme A.

efficiencies of the grate cooler, which vary between 83.20% and 84.86%, when the inlet temperature of cooling air increases from 30°C to 100°C.

5.3 Optimization of scheme B

In scheme B, the exhaust air is induced into chamber 1.

Similar to scheme A, eight subschemes are optimized according to different inlet temperatures of the cooling air, varying from 30°C to 100°C with 10°C intervals. Further, the final optimal cooling air distribution of each subscheme is decided according to the energy consumed by the cooling fans minimization, as shown in Table 3. Figure 9(a) presents the variation in minimum energy consumption of cooling fans with cooling-air inlet temperature in scheme B. The minimum energy consumption of cooling fans is observed to have a subtle change, which is no more than 4% with the increase in inlet temperature of cooling air. The definition of the thermal efficiency of a grate cooler is the same as that mentioned in Section 5.2. Moreover, Figure 9(b) shows the variation in the thermal efficiency of a grate cooler with inlet temperature of cooling air. The thermal efficiencies of the grate cooler vary slightly from 83.25% to 83.76% with different inlet temperatures of cooling air.

6 Discussion

The radiative heat transfer between clinker particles and cooling air is not considered in this study. Moreover, the quenching zone is located in the front of grate plate 1. According to the optimization results, the clinker is already cooled under 600°C at the end of clinker stage 2. Therefore, the radiative heat transfer can be ignored in most parts of the grate cooler. The optimization results agree with the actual measurements, especially in the high-temperature zone. This ensures the temperatures of secondary and tertiary air. Therefore, to simplify the study, convective and conductive heat transfer coefficients between clinker particles and cooling air are considered only.

The thermal load is decided by the overall inlet and outlet temperature differences of hot clinkers in the grate cooler. The inlet temperature of hot clinkers is the same for both schemes A and B. The variations in clinker outlet tempera-

Table 3 Optimal air distribution of subschemes in scheme B

Cooling air temperature (°C)	Mass flow rate of chamber 1 (kg/s)	Mass flow rate of chamber 2 (kg/s)	Mass flow rate of chamber 3 (kg/s)	Mass flow rate of chamber 4 (kg/s)	Mass flow rate of chamber 5 (kg/s)	Mass flow rate of chamber 6 (kg/s)	Mass flow rate of chamber 7 (kg/s)	Mass flow rate of chamber 8 (kg/s)	Mass flow rate of chamber 9 (kg/s)
30	25.05	22.02	30.93	18.45	23.45	18.90	12.86	12.33	12.89
40	24.01	19.99	32.59	20.38	24.31	18.64	12.29	15.00	14.64
50	25.20	21.43	31.27	18.64	23.90	19.81	11.94	14.34	13.85
60	24.01	22.80	31.11	18.56	25.47	19.12	9.85	17.33	12.55
70	25.26	21.28	28.77	20.89	25.74	20.67	14.35	16.15	11.64
80	24.83	21.95	30.53	19.46	24.71	20.81	13.80	14.55	14.32
90	27.11	21.16	30.59	20.32	24.19	18.37	12.78	14.94	12.70
100	26.55	21.57	30.12	20.30	26.08	17.21	12.34	12.70	13.36

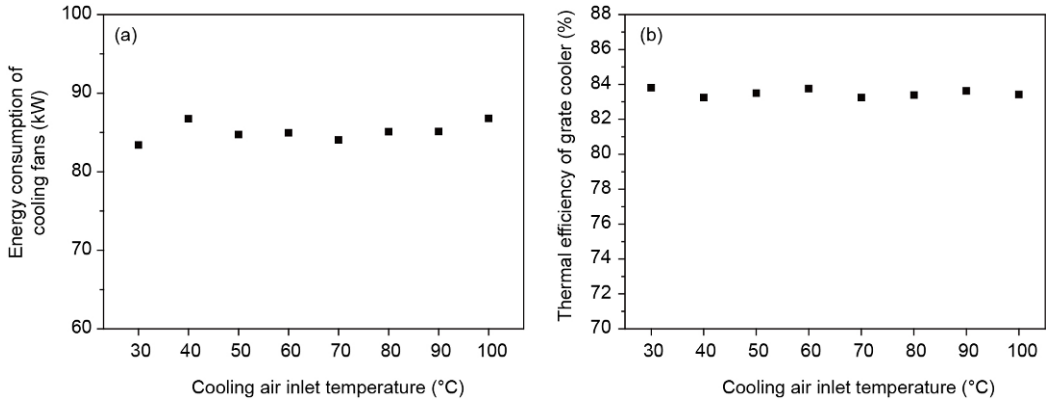

Figure 9 The variation of two key parameters. (a) Minimum energy consumption of cooling fans; (b) thermal efficiency of grate cooler with cooling air inlet temperature in scheme B.

tures of the grate cooler with the cooling air inlet temperatures in schemes A and B are shown in Figure 10. Under all the subscheme conditions, the clinker outlet temperatures of the grate cooler vary slightly from 77.74°C to 85.60°C for scheme A and 80.20°C to 85.18°C for scheme B. It is predicted that the thermal loads undertaken by cooling air distribution are basically the same.

6.1 Energy consumption of cooling fans

As mentioned earlier, the difference between schemes A and B is the location of inducing the exhaust air. For scheme A, the exhaust air was induced in the middle part, that is, chambers 3–6, and the average temperature of clinker particles above these chambers is approximately 250°C, whereas the average temperature of clinker particles of scheme B is normally above 800°C. From the point of view of convection of heat transfer principle, for scheme A, there is a small temperature difference between clinker particles and cooling air, and increasing the inlet temperature of cooling air greatly influences the performance of convection heat transfer. With the same thermal loads, more air volumes are needed to decrease the temperature difference (Figure 11), which leads to the increment of energy consumption of cooling fans, as shown in Figure 8. However, for scheme B, the temperature difference between clinker particles and cooling air is much larger; thus, increasing the inlet temperature of cooling air in the front part of the grate cooler slightly influences the performance of convection heat transfer. The air volumes remain the same (Figure 11**)**. Therefore, energy consumption of cooling fan varies slightly (Figure 9**)** while inducing the exhaust air to chamber 1.

6.2 Thermal efficiency of grate cooler

From the point of view of thermal efficiency of the grate cooler, increasing the cooling air inlet temperature will increase the total heat of the system. This will decrease the thermal efficiency of the grate cooler, according to the definition. However, the thermal efficiencies of the grate cooler basically remain the same for subschemes of both schemes A and B, as shown in Figures 8(b) and 9(b). Notably, the results agree with the goal of optimization. The objective functions

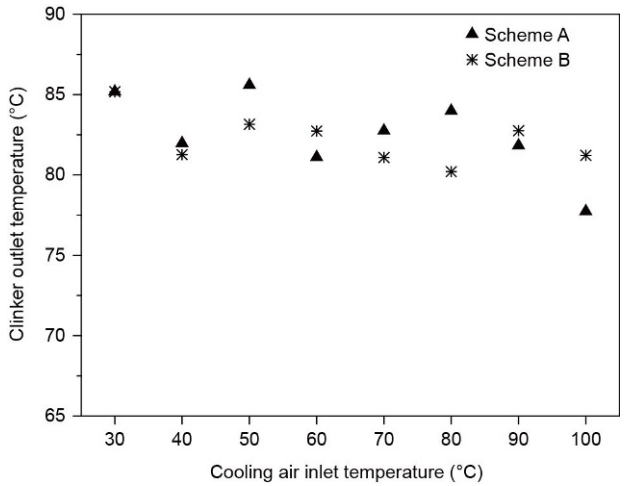

Figure 10 Clinker outlet temperature of grate cooler with cooling air inlet temperature in schemes A and B.

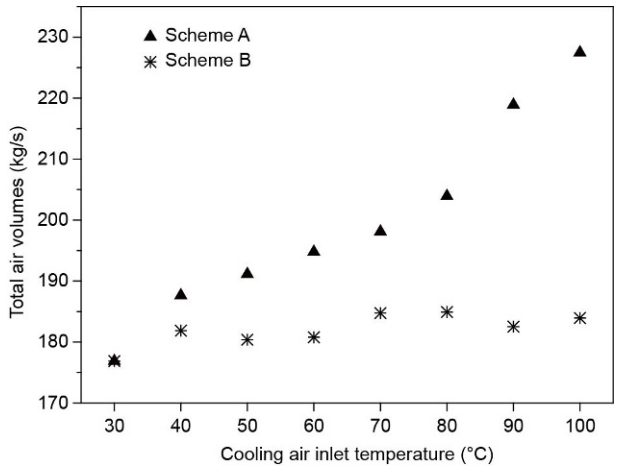

Figure 11 Variation of total air volume with cooling air inlet temperature in schemes A and B.

ensure minimum entropy generation during the heat transfer and flowing process with varying cooling-air inlet temperatures. Therefore, the thermal efficiencies of the grate cooler are similar under all the subschemes conditions. That is, instead of using multiobjective optimizations with thermal efficiency and fan power, selecting entropy generation minimization as the objective function causes the least irreversible loss and obtains best performance of heat transfer and flowing process. Thus, to decide the final Pareto optimal solutions, the minimum energy consumption of cooling fans is considered as a criterion for energy conservation.

6.3 Comparisons

As displayed in Figure 8, the minimum energy consumption of cooling fans increases by approximately 121.04% while the cooling air inlet temperature increases from 30°C to 100°C. That is, instead of conserving energy, scheme A consumes more energy through cooling fans to ensure the cooling efficiency. Therefore, inducing exhaust air to the middle part of the grate cooler through the chimney is obviously not economical.

However, the minimum energy consumption of cooling fans varies slightly when the inlet temperature of cooling air increases from 30°C to 100°C in scheme B. An important function of the grate cooler is to recover the exhaust air from the middle part for cogeneration (Figure 1). Therefore, as previously discussed, heat recovery efficiency is the third criterion to be considered. By assuming that heat flowing to the heat recovery boiler is the exhaust air from chambers 3–6, the heat recovery efficiency is defined as the ratio of the heat flowing into the heat recovery boiler to the total heat flowing into the system. Furthermore, Figure 12 presents the variation in the heat recovery efficiencies with the inlet temperature of cooling air. The heat recovery efficiency is observed to slightly vary between 36.83% and 39.19%, while the inlet temperature of cooling air increases. In conclusion, under the analyses of the optimal air distribution of the subschemes of scheme B, all the conditions process similar thermal efficiencies of the grate cooler, energy consumption of cooling fans, and heat recovery efficiencies. In other words, the optimal air distribution ensures cooling efficiency with no additional power consumption by the cooling fans while recovering exhaust air in the chimney at any temperature. Therefore, scheme B is more effective and economical for recovering exhaust air from the chimney.

7 Conclusions

In this study, a multi-objective optimization model was used for obtaining the optimal cooling air distribution of a grate cooler. Two schemes of inducing exhaust air in the chimney to cool the clinker were investigated.

Scheme A induced exhaust air into the middle part of the grate cooler. The minimum energy consumption of cooling fans increased by 121.04% and the thermal efficiencies of the grate cooler varied no more than 1.66% while the cooling air temperature increased from 30°C to 100°C with 10°C intervals. Scheme B induced exhaust air into the front part of the grate cooler. The minimum energy consumption of cooling fans varied slightly and the thermal efficiencies of the grate cooler varied no more than 0.51% while the cooling air temperature increased from 30°C to 100°C with 10°C intervals. Furthermore, scheme B is more economical and effective at any temperature.

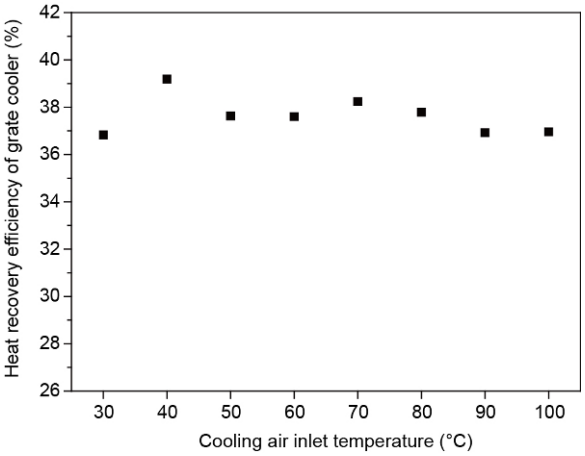

Figure 12 Variation of heat recovery efficiency with cooling air inlet temperature in scheme B.

In future studies, the application of a model will be considered. This will include parameter adjustments for a cement plant with different productive capacities and realization of optimal cooling air distribution.

This work was supported by the National Basic Research Program of China (Grant No. 2013CB228305).

1 Wang J, Dai Y, Gao L. Exergy analyses and parametric optimizations for different cogeneration power plants in cement industry. Appl Energy, 2009, 86: 941–948
2 Li N, Ma D, Chen W. Quantifying the impacts of decarbonisation in China's cement sector: A perspective from an integrated assessment approach. Appl Energy, 2017, 185: 1840–1848
3 Zhang S, Worrell E, Crijns-Graus W. Evaluating co-benefits of energy efficiency and air pollution abatement in China's cement industry. Appl Energy, 2015, 147: 192–213
4 Caputo A C, Pelagagge P M. Heat recovery from moving cooling beds: Transient modeling by dynamic simulation. Appl Thermal Eng, 1999, 19: 21–35
5 Touil D, Belaadi S, Frances C. Energy efficiency of cement finish grinding in a dry batch ball mill. Cement Concrete Res, 2006, 36: 416–421
6 Madlool N A, Saidur R, Hossain M S, et al. A critical review on energy use and savings in the cement industries. Renew Sustain Energy Rev, 2011, 15: 2042–2060
7 Liu Z, Wang Z, Yuan M Z, et al. Thermal efficiency modelling of the cement clinker manufacturing process. J Energy Inst, 2015, 88: 76–86

8 Ahmadi P, Dincer I. Thermodynamic and exergoenvironmental analyses, and multi-objective optimization of a gas turbine power plant. Appl Thermal Eng, 2011, 31: 2529–2540
9 Ghaebi H, Saidi M H, Ahmadi P. Exergoeconomic optimization of a trigeneration system for heating, cooling and power production purpose based on TRR method and using evolutionary algorithm. Appl Thermal Eng, 2012, 36: 113–125
10 Zheng J H, Chen J J, Wu Q H, et al. Multi-objective optimization and decision making for power dispatch of a large-scale integrated energy system with distributed DHCs embedded. Appl Energy, 2015, 154: 369–379
11 Mamaghani A H, Najafi B, Shirazi A, et al. Exergetic, economic, and environmental evaluations and multi-objective optimization of a combined molten carbonate fuel cell-gas turbine system. Appl Thermal Eng, 2015, 77: 1–11
12 Falke T, Krengel S, Meinerzhagen A K, et al. Multi-objective optimization and simulation model for the design of distributed energy systems. Appl Energy, 2016, 184: 1508–1516
13 Seijo S, del Campo I, Echanobe J, et al. Modeling and multi-objective optimization of a complex CHP process. Appl Energy, 2016, 161: 309–319
14 Ahmadi M H, Ahmadi M A, Bayat R, et al. Thermo-economic optimization of Stirling heat pump by using non-dominated sorting genetic algorithm. Energy Conv Manage, 2015, 91: 315–322
15 Ahmadi M H, Ahmadi M A, Mehrpooya M, et al. Thermo-ecological analysis and optimization performance of an irreversible three-heat-source absorption heat pump. Energy Conv Manage, 2015, 90: 175–183
16 Sahraie H, Mirani M R, Ahmadi M H, et al. Thermo-economic and thermodynamic analysis and optimization of a two-stage irreversible heat pump. Energy Conv Manage, 2015, 99: 81–91
17 Caputo A C, Cardarelli G, Pelagagge P M. Analysis of heat recovery in gas-solid moving beds using a simulation approach. Appl Thermal Eng, 1996, 16: 89–99
18 Caputo A C, Pelagagge P M. Economic design criteria for cooling solid beds. Appl Thermal Eng, 2001, 21: 1219–1230
19 Bejan A. Entropy Generation Through Heat and Fluid Flow. New York: John Wiley and Sons Press, 1982
20 Bejan A. Second law analysis in heat transfer. Energy, 1980, 5: 720–732
21 Hesselgreaves J E. Rationalisation of second law analysis of heat exchangers. Int J Heat Mass Transfer, 2000, 43: 4189–4204
22 Yilmaz M, Sara O N, Karsli S. Performance evaluation criteria for heat exchangers based on second law analysis. Exergy An Int J, 2001, 1: 278–294
23 Guo J F. Thermodynamic Analysis and Optimization Design of Heat Exchanger. Dissertation for Doctoral Degree. Jinan: Shandong University, 2011
24 Hu D H. Gas-Solid Process Engineering and Application in Cement Industry. Wuhan: Wuhan University of Technology Press, 2003
25 Wang L, Deng L, Ji C, et al. Multi-objective optimization of geometrical parameters of corrugated-undulated heat transfer surfaces. Appl Energy, 2016, 174: 25–36